Control of Fur synthesis by the non-coding RNA RyhB and iron-responsive decoding

Branislav Večerek[1], Isabella Moll[1] and Udo Bläsi*

Department of Microbiology and Immunobiology, Max F Perutz Laboratories, University of Vienna, Vienna, Austria

The Fe^{2+}-dependent Fur protein serves as a negative regulator of iron uptake in bacteria. As only metallo-Fur acts as an autogeneous repressor, Fe^{2+} scarcity would direct *fur* expression when continued supply is not obviously required. We show that in *Escherichia coli* post-transcriptional regulatory mechanisms ensure that Fur synthesis remains steady in iron limitation. Our studies revealed that *fur* translation is coupled to that of an upstream open reading frame (*uof*), translation of which is downregulated by the non-coding RNA (ncRNA) RyhB. As RyhB transcription is negatively controlled by metallo-Fur, iron depletion creates a negative feedback loop. RyhB-mediated regulation of *uof-fur* provides the first example for indirect translational regulation by a *trans*-encoded ncRNA. In addition, we present evidence for an iron-responsive decoding mechanism of the *uof-fur* entity. It could serve as a backup mechanism of the RyhB circuitry, and represents the first link between iron availability and synthesis of an iron-containing protein.

Introduction

Iron is required as a cofactor for a large number of enzymes, and thus is pivotal for cellular metabolism. In contrast, under oxygen-rich conditions, iron is a source of toxic radicals, which can damage cellular components. Therefore, bacteria have evolved fine-tuned regulatory systems, which on one hand ensure sufficient iron uptake, and on the other hand minimize iron toxicity (Escolar *et al*, 1999; Hantke, 2001; Kadner, 2005). The *f*erric *u*ptake *r*egulator Fur is a key regulator of iron metabolism (Hantke, 1984). In the presence of Fe^{2+}, metallo-Fur binds as a dimer to iron-responsive promoter regions termed Fur-boxes and blocks the access of RNA polymerase (Escolar *et al*, 1999). In contrast, gene induction by metallo-Fur has remained puzzling until Massé

*Corresponding author. Department of Microbiology and Immunobiology, Max F Perutz Laboratories, University of Vienna, Dr. Bohrgasse 9/4, Vienna 1030, Austria.
Tel.: +43 1 4277 54609; Fax: +43 1 4277 9546;
E-mail: udo.blaesi@univie.ac.at
[1]These authors equally contributed to this work

and Gottesman (2002) showed that transcription of the *non-*coding RNA (ncRNA) RyhB is negatively controlled by metallo-Fur, and that RyhB downregulates the expression of genes encoding iron-containing proteins. These authors proposed that RyhB blocks ribosome binding to the respective mRNA(s) through base-pairing. This hypothesis was supported by studies of the *sodB* gene encoding FeSOD, the iron-containing superoxide dismutase (Večerek *et al*, 2003; Geissmann and Touati, 2004). Moreover, blockage of *sodB* mRNA translation by RyhB was shown to result in rapid turnover of both the mRNA and the ncRNA (Massé *et al*, 2003; Afonyushkin *et al*, 2005; Morita *et al*, 2006).

Despite the central role of Fur in iron metabolism and virulence in several bacterial pathogens (Braun, 2005), the mechanisms governing *fur* expression are not fully understood. The primary regulators of the oxidative stress response, OxyR and SoxRS, stimulate *Escherichia coli fur* transcription from different promoters, which complies with the function of Fur in protecting cells against oxidative damage (Zheng *et al*, 1999). Autogeneous regulation by binding of metallo-Fur to its own promoter has been reported in several bacteria (Delany *et al*, 2002; Sala *et al*, 2003; Hernandez *et al*, 2006), and *E. coli fur* expression is known to be moderately auto-regulated (De Lorenzo *et al*, 1988). However, a remaining paradox in *fur* auto-repression is that only metallo-Fur is able to bind efficiently to Fur-boxes, that is, the transition from iron-replete to iron-deplete conditions would lead to transcription of *fur* under conditions where Fur requirement is not obvious.

In this study, we have tested whether *fur* gene expression is post-transcriptionally regulated in *E. coli*. We show that Fur synthesis is translationally coupled to that of an upstream open reading frame, which hereafter is termed *uof* (*u*pstream *o*f *fur*), and that the ncRNA RyhB downregulates translation of *uof*. Moreover, evidence is presented for iron-responsive decoding of *uof*. The key features of this novel mechanism involve decoding of the Ser codon UCA by $tRNA_{IV}^{Ser}$ and an adjacent rare Arg codon.

Results

RyhB affects the abundance and stability of fur mRNA

Overexpression of the *hfq* RNA chaperone gene led to an increase in RyhB levels and to a concomitant decrease in the levels of *fur* mRNA (Večerek *et al*, 2003), indicating a possible role of RyhB in the post-transcriptional control of *fur*. We first verified this observation by determining the steady-state levels of *fur* mRNA in an *E. coli ryhB−* strain and in the parental strain upon addition of the iron chelator 2,2′-dipyridyl (dip), which is known to induce *ryhB* transcription by alleviating the negative control of Fur (Massé and Gottesman, 2002). The levels of *fur* mRNA increased during a time course of 16 min after addition of dip in the *ryhB−* mutant, whereas they did not significantly change in the *ryhB+* strain (Figure 1A and B). One possible explanation for this observation was
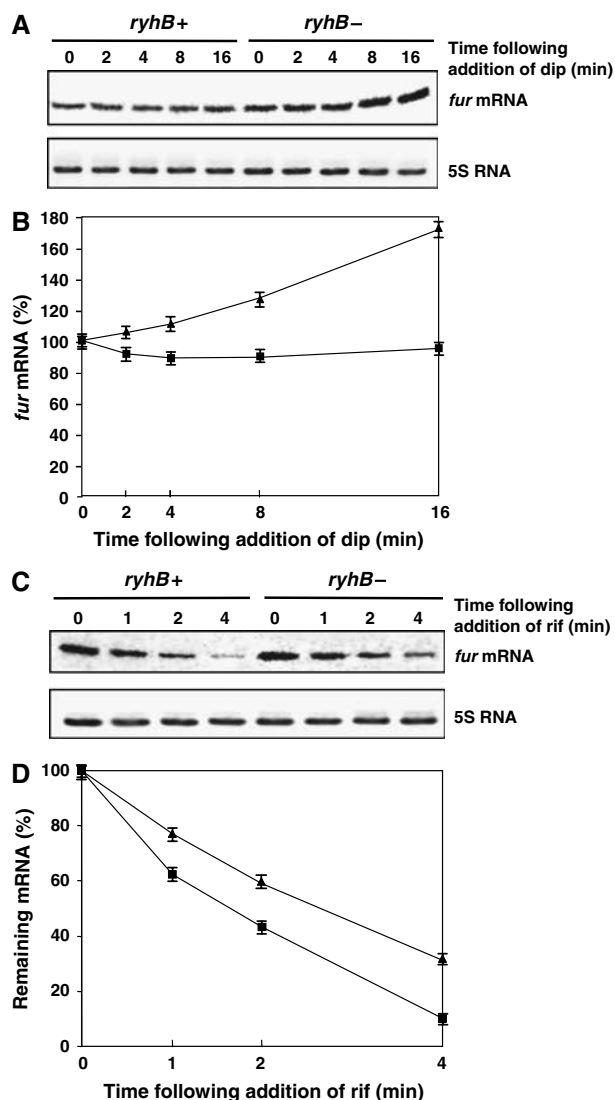
Figure 1 RyhB negatively affects the steady-state levels and stability of *fur* mRNA. (**A**) Steady-state levels of *fur* mRNA upon addition of the iron chelator 2,2′-dipyridyl (dip) to exponentially growing cultures of *E. coli* DJ480 (*ryhB+*) and the isogenic Δ*ryhB* (*ryhB−*) strain. Total RNA was extracted before (time 0) and several times after addition of dip as indicated, and the steady-state levels of *fur* mRNA and 5S rRNA (internal control) were determined by primer extension. (**B**) Graphical representation of the *fur* mRNA levels at different times after addition of dip in the *ryhB+* (■) and the *ryhB−* (▲) strain. The signals shown in the autoradiograph (A) were quantified by the ImageQuant software and the *fur*-specific signals were normalized to that of 5S rRNA. The signal intensities obtained at time 0 were set to 100%. (**C**) Stability of *fur* mRNA in the presence and absence of RyhB. Total RNA was extracted from exponentially growing *ryhB+* and *ryhB−* strains before (time 0) and several times after addition of rifampicin. The amount of *fur* mRNA and 5S rRNA at each time was determined as described in Materials and methods. (**D**) The *fur* and 5S rRNA-specific signals (C) were quantified and the *fur*-specific signals were normalized to 5S rRNA. The relative amount of *fur* mRNA remaining at each time point in the *ryhB+* (■) and *ryhB−* (▲) strains is plotted as a function of time. The signal intensities obtained at time 0 were set to 100%. The experiments were performed in duplicate. The relevant sections of representative autoradiographs are shown in (A) and (C). Error bars (B, D) represent s.d.

that the absence of RyhB results in higher levels of iron-containing proteins (Massé *et al*, 2005), which would decrease the cellular Fe^{2+} pool, leading to a reduced Fur

activity, which in turn could result in derepression of *fur* transcription. Another explanation was that RyhB negatively regulates *fur* expression by directly affecting the stability of the transcript. The stability of *fur* mRNA was determined in the presence and absence of RyhB. The strains were grown to an OD_{600} of 0.5, treated with rifampicin, and the *fur* mRNA levels were determined several times thereafter. As shown in Figure 1C and D, when compared with the parental strain ($t_{1/2} \sim 1.6$ min) the stability of *fur* mRNA was significantly increased in the *ryhB−* strain ($t_{1/2} \sim 2.5$ min). These experiments suggested that RyhB somehow counterbalances the increasing *fur* transcript levels, which under conditions of iron-depletion, results from a lack of metallo-Fur.

Features of the 5′-untranslated region suggest a mechanism for indirect post-transcriptional control of fur by RyhB

As ncRNAs can prevent ribosome loading, which is followed by degradation of both the mRNA and the ncRNA (Massé *et al*, 2003), we searched for a possible RyhB target site in the vicinity of the *fur* ribosome binding site (rbs). However, an obvious complementarity between RyhB and the *fur* translation initiation region was not apparent. When transcribed from its authentic promoter, the *E. coli fur* transcript starts at nt −183 with regard to the A (nt +1) of the *fur* mRNA start codon (Zheng *et al*, 1999). We noticed that the *fur* transcript comprises an open reading frame (*uof*), which consists of 28 codons. It is located immediately upstream of and overlaps with the 5′-coding region of the *fur* gene (Figure 2). An extended complementarity between RyhB and the putative translation initiation region of *uof* was revealed by bioinformatics (Figure 2). In addition, we noted that the Shine and Dalgarno (SD) sequence of *fur* mRNA is masked by a putative stem–loop structure (Figure 2). Given that *uof* translation was predicted to be terminated at either of the two consecutive stop codons in the immediate coding region of *fur* mRNA, we next addressed the questions whether translation of *fur* is positively coupled to that of *uof*, and whether negative regulation of *fur* by RyhB could be exerted through inhibition of *uof* translation.

fur translation is coupled to that of uof

As a canonical SD sequence was not apparent for *uof* (Figure 2), we first tested by *in vitro* toeprinting whether ribosome binding occurs at its putative start codon. As shown in Figure 3A, lane 3, a 30S ternary complex formed over the predicted start codon of *uof* (AUG_{uof}) and *fur* (AUG_{fur}), respectively. Two primer extension inhibition signals were obtained as a result of ribosome binding at AUG_{fur}, which was indicative of sub-optimal 30S ribosome binding (Bläsi *et al*, 1989). Therefore, the structure of *uof-fur* mRNA comprising the region upstream of AUG_{fur} was mapped by enzymatic probing. This analysis supported the idea that the *fur* SD sequence is occluded by a stem–loop structure (Figure 2 and Supplementary Figure S1), which in turn underlined the possibility that *fur* translation is coupled to that of *uof*.

Several plasmids were constructed to test this hypothesis *in vitro* and *in vivo*. In all constructs, the *lacpo* (pR series) and *lacpo* or T7-promoter (pU series)-driven transcript encompasses *uof-fur* mRNA starting at nt −183 (Figure 2). The plasmid pair pUuof$_{AUG}$fur/pUuof$_{UA-CUG}$fur (Figure 3B) is identical except that the AUG start codon of *uof* was changed
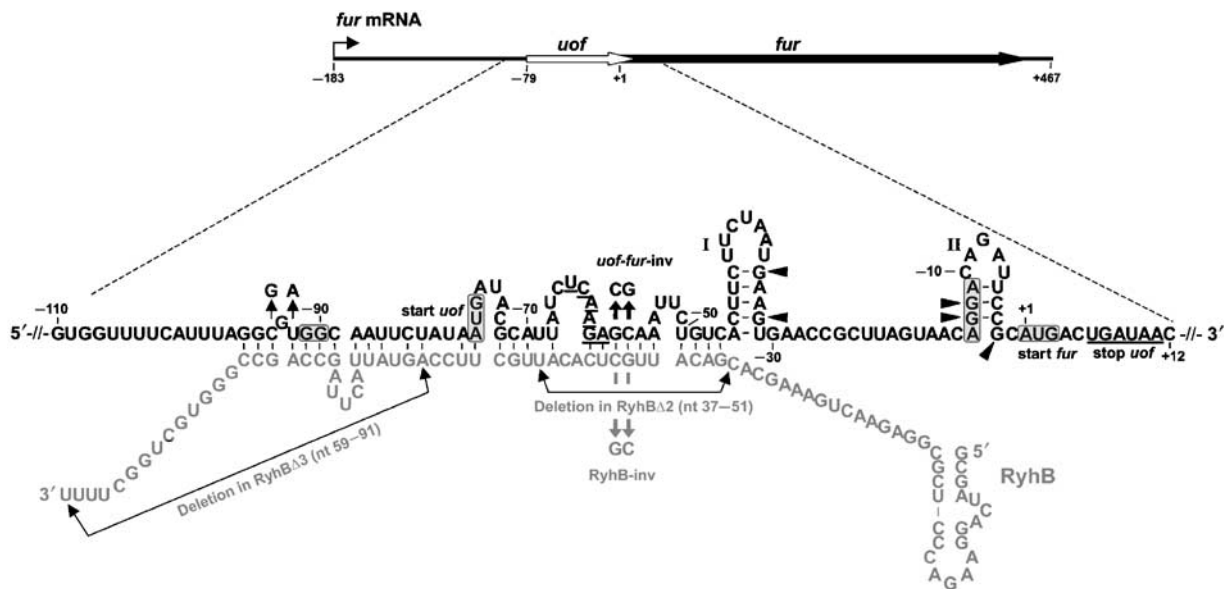
Figure 2 Organization of *fur* mRNA and base-pairing between *uof* and RyhB. The *uof* and *fur* reading frames are depicted by white and black arrows, respectively. The sequence comprising nt −110 to +12 is enlarged. The putative SD sequences and start codons of *uof* and *fur* are boxed. The -GG- to -GGAGG- mutation in the putative SD of *uof* is indicated (see Figure 3C). The *uof* codons UCA$_6$ and AGA$_7$ involved in iron-responsive decoding (see text) and the two consecutive stop codons of *uof* in the proximal coding region of the *fur* gene are underlined. The stem–loop structures I and II were revealed by enzymatic probing (see Supplementary Figure S1). Bases protected from RNase T1 are indicated by filled arrowheads. The potential base-pairing between *uof-fur* mRNA and RyhB RNA is depicted. Analysis of complementarity was performed using the SeqMan software (Lasergene, DNA Star Inc.). The deletions made in the RyhB variants RyhBΔ2 and RyhBΔ3 are indicated. The mutations introduced in *uof* (pUuof$_{AUG}$fur-inv) and RyhB (RyhB-inv) are denoted by arrows.

to a CUG and the -GG- bases, comprising the putative SD sequence of *uof* (Figure 2), were changed to -UA-. This was carried out with the reasoning that abrogation of *uof* translation should either drastically reduce or prevent translation of the *fur* gene. The removal of the translation initiation signals of *uof* abolished concurrent *in vitro* translation of the *fur* gene (Figure 3B, lane 2). Similarly, Fur synthesis did not occur upon *in vitro* translation of a *fur* mRNA variant bearing a UGA stop codon at position 6 in *uof* (Figure 3B, lane 3), that is, the premature stop codon in *uof* appeared to prevent translational coupling at the *uof-fur* boundary. The stop codons of *uof* are situated two nucleotides downstream of the *fur* start codon (see Figure 2). To test whether this putative 'termination-restart motif' (Pavlov *et al*, 1997) is required for translational coupling at the *uof-fur* junction, the two stop codons of *uof* were replaced by sense codons (Figure 3B), and the *fur* mRNA variant was translated *in vitro*. The replacement of the *uof* stop codons drastically reduced *fur* translation and resulted in the synthesis of an *uof*-specific polypeptide (Figure 3B, lane 4; P73), which terminated at an in-frame stop codon located 73 codons downstream of the *uof* start codon. This experiment indicated that termination at the *uof* stop codon(s) is required for translation initiation of *fur*.

In contrast to the *E. coli* MC4100 harboring plasmid pRuof$_{AUG}$fur-lacZ (wild-type (wt) *uof-fur* entity; Figure 3C, lane 2), synthesis of the FurΦLacZ fusion protein was not observed *in vivo* in strains bearing plasmids pRuof$_{CUG}$fur-lacZ (Figure 3C, lane 3) and pRuof$_{UA-CUG}$fur-lacZ (Figure 3C, lane 5), in which the *uof* start codon was replaced by CUG and both the putative SD sequence and the start codon were altered, respectively. Similarly, when only the putative SD sequence -GG- of *uof* was changed to -UA-, synthesis of the

UofΦLacZ protein was greatly diminished (Figure 3C, lane 4). Again, this set of *in vivo* experiments showed that translation of *uof* is required for concomitant translation of *fur*. To verify these observations, we also tested whether altering the weak SD sequence, -GG-, of *uof* to the canonical SD sequence -GGAGG- would result in enhanced translation of the *fur* reading frame. When compared with the authentic -GG- sequence, this modification increased FurΦLacZ synthesis ∼3.5-fold (Figure 3C, lane 6), which clearly supported the hypothesis that *fur* translation is coupled to that of *uof*. Moreover, the fusion proteins UofΦLacZ and FurΦLacZ, encoded by plasmids pRuof-lacZ and pRuof$_{AUG}$fur-lacZ, respectively, were synthesized at a comparable level (Figure 3C, lanes 1 and 2), suggesting that a translational termination event in *uof* results in a translational restart at the *fur* start codon. In summary, the data presented in Figure 3 revealed that translation of the distal *fur* gene depends on translation of the proximal *uof* reading frame.

We also tested whether the lack of *uof* translation affects the stability of *uof-fur* mRNA in strains H1941Δ*fur*(pUuof$_{AUG}$fur) and H1941Δ*fur*(pUuof$_{UA-CUG}$fur). When compared with *uof*$_{AUG}$*fur* mRNA ($t_{1/2}$ ∼1.9 min), removal of the translation initiation signals in *uof*$_{UA-CUG}$*fur* mRNA resulted in greatly reduced steady-state levels as well as in a faster decay of the *uof*$_{UA-CUG}$*fur* mRNA ($t_{1/2}$ ∼0.6 min) *in vivo* (Supplementary Figure S2).

RyhB downregulates the translation of uof and thereby Fur synthesis

Next, we asked whether post-transcriptional regulation of *fur* entails translational repression of *uof* by RyhB, and consequently that of the *fur* gene. First, we employed plasmid pRuof-lacZ (see Figure 3C), encoding an *uof-lacZ* fusion to
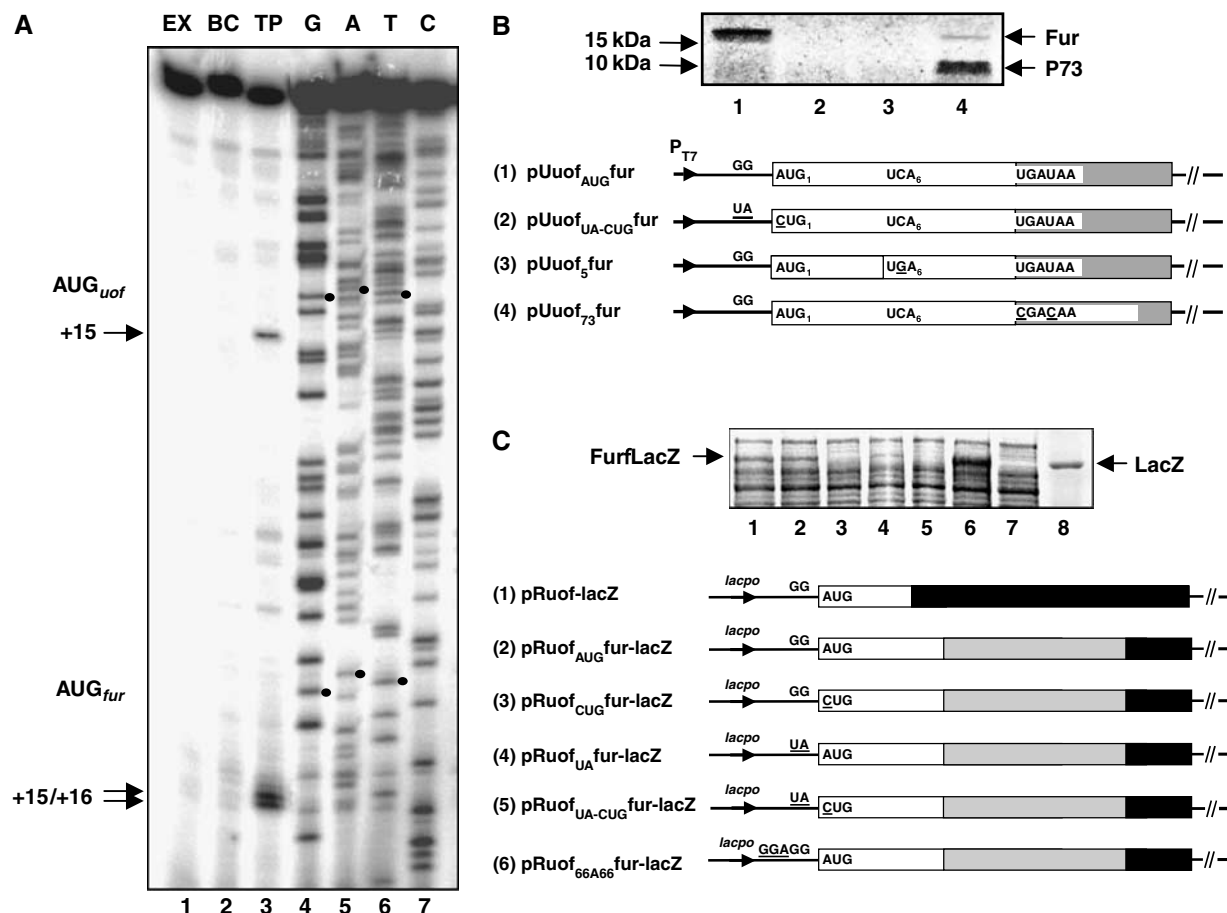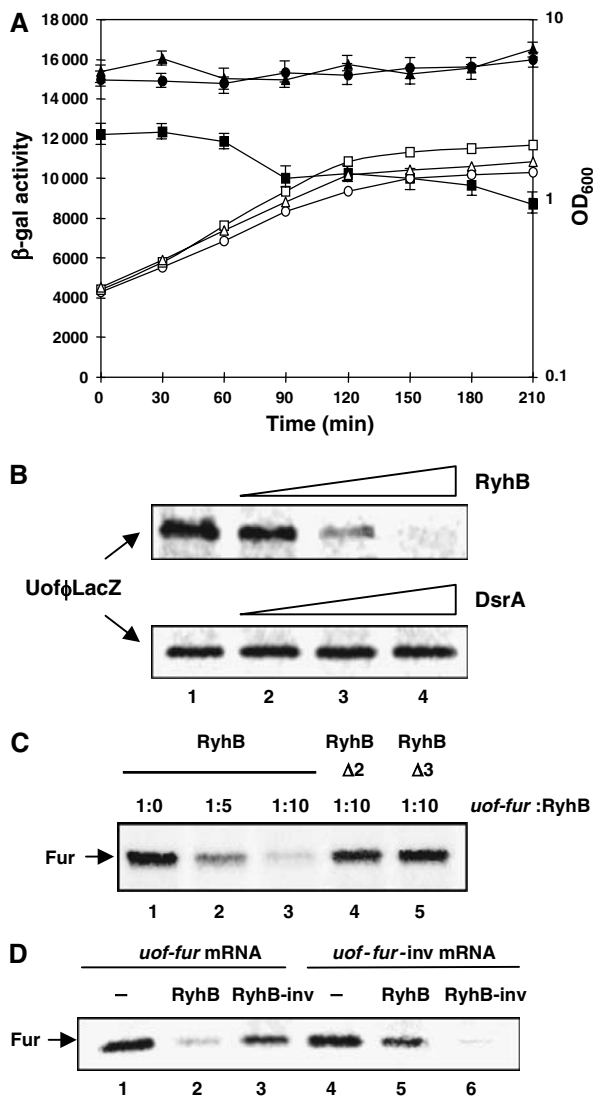
Figure 3 Coupled translation of *uof* and *fur*. (**A**) Toeprinting of *fur*242 mRNA. Lane 1: primer extension (EX) in the absence of 30S ribosomal subunits and tRNA$_f^{Met}$, lane 2: primer extension in the presence of 30S subunits (binary complex, BC), lane 3: toeprinting (TP) in the presence of 30S subunits and tRNA$_f^{Met}$, lanes 4–7: sequencing reactions. Arrows denote the primer extension inhibition signals as a result of ternary complex formation at the start codon of *uof* (AUG$_{uof}$) and the *fur* gene (AUG$_{fur}$). The dots in the autoradiograph depict the positions of the *uof* and *fur* start codons. (**B**) The full-length 'wild-type' and mutant *fur* mRNAs were transcribed *in vitro* from the corresponding plasmids, as shown schematically below the autoradiograph. The *uof* and *fur* genes are depicted by white and gray bars, respectively. Mutations created in the translation initiation signals, the coding sequence and the stop codons of *uof* at the mRNA level are underlined. Equimolar concentrations (400 nM) of the respective *fur* mRNAs were used to program the *in vitro* translation reactions. The ^{14}C-labeled translation products were resolved by SDS–polyacrylamide gel electrophoresis. Lanes 1–4: *in vitro* translation of *fur* mRNAs derived from plasmids pUuof$_{AUG}$-fur (1), pUuof$_{UA−CUG}$-fur (2), pUuof$_5$-fur (3) and pUuof$_{73}$-fur (4), respectively. The positions of the $\sim$17-kDa Fur protein and the *uof*-specific 73-aa product (P73) are indicated by arrows on the right. The positions of marker proteins and their molecular masses in kDa are shown by arrows on the left. (**C**) The *E. coli* MC4100 harboring plasmid pRuof-lacZ (1), wherein the first 24 codons of *uof* are fused to the 8th codon of the *lacZ* gene, or plasmids pRuof$_{AUG}$fur-lacZ (2), pRuof$_{CUG}$fur-lacZ (3), pRuof$_{UA}$fur-lacZ (4), pRuof$_{UA-CUG}$fur-lacZ (5) or pRuof$_{GGAGG}$fur-lacZ (6), wherein the first 36 codons of the *fur* gene are fused to the 8th codon of the *lacZ* gene, respectively, was grown in M9 medium to an OD$_{600}$ of 0.5. Then, 1 ml aliquots of the respective cultures were pulse labeled with [^{35}S]methionine for 2 min. Lane 1: UofΦLacZ protein synthesized in strain MC4100(pRuof-lacZ), lanes 2–6: FurΦLacZ proteins synthesized in strains MC4100(pRuof$_{AUG}$fur-lacZ; wt *uof-fur* entity), MC4100(pRuof$_{CUG}$fur-lacZ; *uof*$_{AUG \to CUG}$), MC4100(pRuof$_{UA}$fur-lacZ: putative SD of *uof* was changed from -GG- to -UA-), MC4100(pRuof$_{UA-CUG}$fur-lacZ; *uof*$_{AUG \to CUG}$ and putative SD of *uof* was changed from -GG- to -UA-) and MC4100(pRuof$_{GGAGG}$fur-lacZ; putative SD of *uof* was changed from -GG-to -GGAGG-), respectively, lane 7: lack of β-galactosidase synthesis in strain MC4100 carrying the parental plasmid pRB381 (control), lane 8: molecular weight marker β-galactosidase. Only the relevant part of the autoradiograph is shown. The position of the FurΦLacZ fusion proteins and that of LacZ are denoted by arrows. The corresponding plasmids (1–6) are schematically shown below the autoradiograph. The *uof*, *fur* and *lacZ* gene(s) are depicted by white, gray and black bars, respectively. Mutations created in the translation initiation signals of *uof* at the mRNA level are underlined.

monitor *uof* translation in the *ryhB+* and the *ryhB−* strain. When compared with the *ryhB−* mutant, a decreased synthesis of the UofΦLacZ protein was seen in the *ryhB+* strain, which became more apparent when the cultures entered the stationary phase (Figure 4A), that is, concomitant with the reported increase in RyhB synthesis (Argaman *et al*, 2001). As RyhB is known to require the RNA chaperone Hfq for function, we also tested whether the observed decrease in synthesis of the UofΦLacZ protein in the presence of RyhB depends on Hfq. When compared with the wt strain, the absence of

Hfq led to a comparable increase in translation of the *uof-lacZ* gene as observed in the absence of RyhB (Figure 4A), suggesting that RyhB-mediated regulation of *uof* depends on Hfq.

Second, to further test whether RyhB inhibits *uof* translation, the *uof-lacZ* gene encoded by the pRuof-lacZ plasmid was expressed in an *E. coli in vitro* transcription/translation system in the presence of increasing concentrations of RyhB. As shown in Figure 4B, increasing concentrations of RyhB either reduced or inhibited *uof-lacZ* expression, whereas increasing amounts of the nonspecific ncRNA DsrA did not.

Figure 4 RyhB inhibits translation of *uof* and concomitantly of *fur*. (**A**) Translation of the *uof-lacZ* fusion gene in the *E. coli ryhB+* (■), *ryhB−* (▲) and *hfq−* (●) strains. All strains harbored plasmid pRuof-lacZ (Figure 3C), wherein the first 24 codons of *uof* are fused to the 8th codon of the *lacZ* gene. The strains were cultivated in M9 medium and triplicate aliquots were taken at different optical densities during growth of the *ryhB+* (□), *ryhB−* (△) and *hfq−* (○) strains. The experiment was performed in duplicate. Error bars represent s.d. (**B**) The coupled *in vitro* transcription/translation reactions were programmed with 4 μg of plasmid pRuof-lacZ (Figure 3C) and carried out in the absence (lane 1) or presence of 20, 40 and 80 pmol (lanes 2–4) of RyhB RNA (upper panel) or DsrA RNA (lower panel). Only the relevant parts of the autoradiographs are presented. (**C**) *In vitro* translation of full-length *uof-fur* (wt) mRNA derived from plasmid pUuof$_{AUG}$fur (Figure 3B) in the presence of RyhB and deletion variants thereof. *Uof-fur* mRNA (400 nM) was *in vitro* translated in the absence (lane 1) and in the presence of 2 μM (lane 2), 4 μM RyhB (lane 3), 4 μM RyhBΔ2 (lane 4) and 4 μM RyhBΔ3 (lane 5). The molar ratios of *uof-fur*:RyhB are indicated on top of the autoradiograph. (**D**) Lanes 1–3: *in vitro* translation of *uof-fur* mRNA (400 nM) derived from plasmid pUuof$_{AUG}$fur (Figure 3B) in the absence (−) and in the presence of 4 μM RyhB and 4 μM RyhB-inv, lanes 4–6: *in vitro* translation of *uof-fur*-inv mRNA (400 nM) derived from plasmid pUuof$_{AUG}$fur-inv (see Supplementary data) in the absence (−) and in the presence of 4 μM RyhB and 4 μM RyhB-inv, respectively.

Third, we examined whether translational silencing of *uof* by RyhB inhibits translational coupling at the *uof-fur* boundary, and thereby Fur synthesis. Full-length *in vitro*-transcribed *uof-fur* mRNA derived from plasmid pUuof$_{AUG}$fur (Figure 3B) was translated *in vitro* in the presence of increasing concentrations of RyhB RNA. As shown in Figure 4C, lanes 2 and 3, increasing amounts of RyhB blocked *fur* mRNA translation. It is worth noting that the decay rates of *fur* mRNA in the *in vitro* translation system were comparable in the presence and absence of RyhB (Supplementary Figure S3), which indicated that inhibition of Fur synthesis results from a RyhB-mediated block of *uof* translation. For verification, two RyhB deletion constructs, RyhBΔ2 and RyhBΔ3 (Figure 2), were used. When compared with RyhB, neither of the RyhB variants with a reduced complementarity to *uof* exerted a notable effect on *fur in vitro* translation (Figure 4C, lanes 4 and 5). To verify the RyhB–*uof* interaction, mutations were introduced in RyhB RNA at nt positions 43 and 44 and in *uof-fur* mRNA at positions −57 and −58 (see Figure 2; RyhB-inv and *uof-fur*-inv). As shown in Figure 4D, lanes 3 and 5, the RyhB-inv and RyhB wt RNAs did not inhibit synthesis of Fur from *uof-fur* wt mRNA and *uof-fur*-inv mutant mRNA, respectively. In contrast, synthesis of Fur from the *uof-fur*-inv mRNA was blocked by RyhB-inv RNA (Figure 4D, lane 6) bearing the compensatory mutations. Taken together, these results showed that RyhB interacts with the *uof* sequence of the *uof-fur* mRNA, thereby blocking translation *uof*, and consequently that of *fur*.

Evidence for regulation of *uof* by iron-responsive decoding

To test whether the observed effects of RyhB on *fur* mRNA levels (Figure 1A) are mirrored in the *de novo* synthesis of Fur protein *in vivo* pulse-labeling experiments were performed. As shown in Figure 5A, upon addition of dip, the *de novo* synthesis of Fur was hardly affected in the *ryhB+* strain during a time course of 20 min, as expected from the observed insignificant changes in the steady-state levels of *fur* mRNA (Figure 1A). In contrast, upon addition of the chelator, Fur synthesis increased up to 8 min in the *ryhB−* strain and then decreased to comparable levels, as observed in the *ryhB+* strain (Figure 5A) even though the *fur* mRNA levels increased under these conditions (see Figure 1A and B).

The only iron–sulfur (Fe–S) enzyme involved in translation is MiaB (Pierrel *et al*, 2002), which participates in methylthiolation of adenosine 37 (A37) of almost all tRNAs that read codons starting with U (UNN), except tRNA$_I^{Ser}$ and tRNA$_V^{Ser}$ (Grosjean *et al*, 1985). A37, next to the anticodon, stabilizes the codon–anticodon interaction by increasing the stacking energy (Lim, 1997), whereas the modification of A37 affects the accuracy of codon reading in the ribosomal A-site (Bouadloun *et al*, 1986). In addition, it was shown that the ms^{2}io^{6}A-37 hypermodification in *Salmonella typhimurium* tRNAs contributes to the decoding efficiency (Esberg and Björk, 1995). As shown in Figure 2, *uof* comprises, at position six, the serine codon UCA, which is decoded by the MiaB-dependent tRNA$_{IV}^{Ser}$. In addition, the AGA codon downstream of UCA in *uof* is decoded by the rare tRNA$_4^{Arg}$. It is known that the presence of AGA codons close to the initiation codon can lead to ribosome stalling and eventually release of mRNA (Gao *et al*, 1997; Cruz-Vera *et al*, 2004). As iron limitation results in a lack of methylthiolation of A37 (Buck and

A Time following
dip addition (min)

B

C
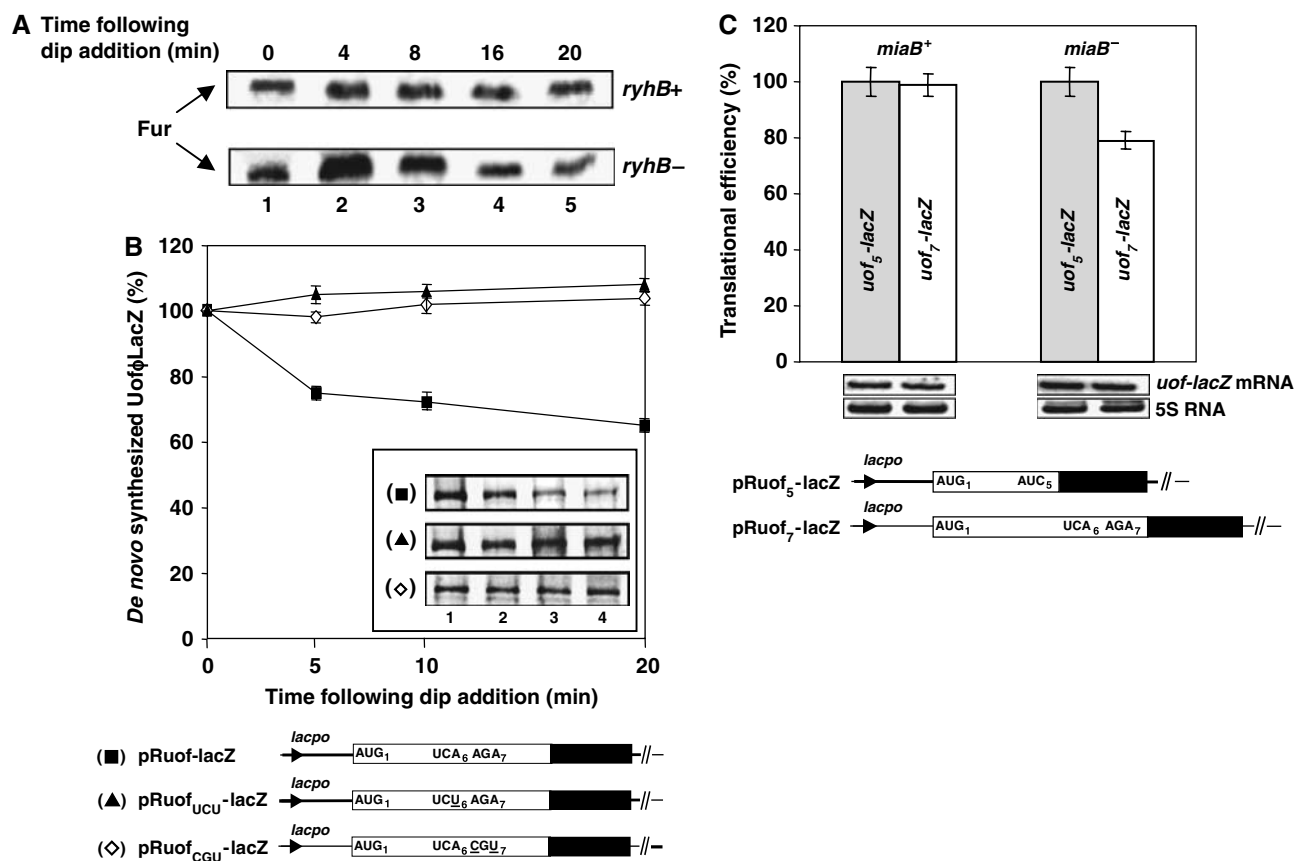
Figure 5 Iron-responsive decoding of *uof*. (**A**) *De novo* synthesis of Fur protein in *E. coli* DJ480 (upper panel) and in the isogenic Δ*ryhB* strain (lower panel) upon addition of the iron chelator dip. The cells were grown in M9 medium to an OD$_{600}$ of 0.5. Aliquots (1 ml) of both cultures were pulse labeled with [^{35}S]methionine (10 mCi/ml) for 2 min before (time 0), 4, 8, 16 and 20 min after addition of dip. The samples were processed as described in Materials and methods. Only the relevant part of the autoradiograph of the immunoblot showing the synthesized Fur protein (arrow) is presented. (**B**) Graphical representation of the *de novo* synthesis of UofΦLacZ protein upon addition of dip in the *E. coli* DJ480Δ*ryhB* harboring plasmids pRuof-lacZ (■), pRuof$_{UCU}$-lacZ (▲) and pRuof$_{CGU}$-lacZ (◇). The experiment was performed in duplicate. Error bars represent s.d. Insert: DJ480Δ*ryhB* harboring plasmids pRuof-lacZ (■), pRuof$_{UCU}$-lacZ (▲) or pRuof$_{CGU}$-lacZ (◇), was pulse labeled with [^{35}S]methionine for 2 min at time 0 (lane 1), 5 min (lane 2), 10 min (lane 3) and 20 min (lane 4) after addition of dip (final concentration 250 μM). The proteins were resolved in a 12% SDS–polyacrylamide gel. Only the relevant part of the autoradiographs of one representative experiment is shown. In all plasmids (bottom), codon 24 of *uof* (open bar) is fused to the eigth codon of the *lacZ* gene (black bar). Mutations introduced in *uof* at the mRNA level are underlined. (**C**) Translational efficiencies of the *uof$_5$-lacZ* and *uof$_7$-lacZ* fusion genes in an *miaB* + (bars on the left) and an *miaB*− strain (bars on the right) harboring plasmids pRuof$_5$-lacZ (gray bar) and pRuof$_7$-lacZ (white bar). The experiment was performed in duplicate as described in Materials and methods. The values obtained with the *uof$_5$-lacZ* construct were set to 100%. The error bars represent s.d. The steady-state levels of the *uof$_5$-lacZ* and *uof$_7$-lacZ* mRNAs, respectively, are shown below the bars. 5S RNA was used as a loading control. The plasmid constructs used in these experiments are schematically shown at the bottom. The open and black bars represent the *uof* and the *lacZ* gene, respectively.

Griffiths, 1982), we asked whether the observed decrease of Fur *de novo* synthesis in the *ryhB*− strain upon iron depletion (Figure 5A) could be attributed to the consecutive 5′-...UCA$_6$AGA$_7$...-3′ codons (Figure 2), that is, whether this codon arrangement in *uof* renders *uof-fur* translation responsive to iron.

We first tested whether iron depletion affects expression of *uof* in the absence of RyhB. Pulse-labeling experiments for 20 min after addition of dip revealed that the *de novo* translation of the *uof-lacZ* gene was reduced in the *ryhB*− strain by ∼25–30% when it contained the authentic 5′-...UCA$_6$AGA$_7$...-3′ codons in *uof* (Figure 5B). However, when UCA$_6$ in *uof* was replaced by the serine codon UCU, which is cognate for the MiaB independent tRNA$_V^{Ser}$, no dip-dependent decrease in the *de novo* synthesis of the UofΦLacZ protein was observed (Figure 5B). We noted that the steady-state levels of *uof-fur* mRNA derived from strain DJ480Δ*ryhB*

(pRuof-lacZ) and DJ480Δ*ryhB* (pRuof$_{UCU}$-lacZ) after 20 min of addition of dip were comparable (data not shown), which suggested that the observed decrease in the UofΦLacZ synthesis in DJ480(pRuof-lacZ) is linked to translation. Comparably, the conversion of AGA codon 7 to the canonical arginine codon CGU abolished dip-dependent decrease of UofΦLacZ synthesis (Figure 5B).

To verify whether the sub-sequence 5′-...UCA$_6$AGA$_7$...-3′ is sufficient for iron-responsive decoding of *uof*, two plasmids, pRuof$_5$-lacZ and pRuof$_7$-lacZ (Figure 5C) were constructed, in which either *uof* codon 5 or codon 7, was abutted to the 8th codon of the *lacZ* gene. Similarly, as observed in the experiments shown in Figure 5B, addition of dip resulted in a decreased synthesis of the Uof$_7$ΦLacZ but not of that of the Uof$_5$ΦLacZ fusion protein in strain DJ480Δ*ryhB*− (data not shown). Translational efficiencies of the *uof$_5$-lacZ* and *uof$_7$-lacZ* genes obtained with plasmids pRuof$_5$-lacZ

and pRuof$_7$-lacZ were comparable in the *miaB+* strain, showing that the sub-sequence 5′-...UCA$_6$AGA$_7$...-3′ has no general negative effect on expression of the corresponding *lacZ* fusion genes under iron-replete conditions (Figure 5C). To test whether the decrease in *uof$_7$-lacZ* expression upon dip addition is linked to MiaB, we next compared the translational efficiencies of the *uof$_5$-lacZ* and *uof$_7$-lacZ* genes in a *miaB−* strain. As shown in Figure 5C, in the mid-logarithmic phase, the translational efficiency of the *uof$_7$-lacZ* gene was ~20% reduced when compared with that obtained with the *uof$_5$-lacZ* gene. As the steady-state levels of the *uof$_5$-lacZ* and *uof$_7$-lacZ* mRNAs were indistinguishable (Figure 5C), this experiment supported the idea that decoding of the sub-sequence 5′-...UCA$_6$AGA$_7$...-3′ is influenced by MiaB.

Under-modification of A37 appears to affect ribosome movement only to a measurable extend when consecutive iron-responsive UNN codons are present in a reading frame (Landick *et al*, 1990) or, as indicative from Figure 5B, when an UNN codon is adjacent to at least one rare codon. Hence, we analyzed a number of *E. coli* mRNAs, including *sodB*, *sdhD*, *acnA*, *fumA* and *bfr* that encode iron-containing enzymes and are negatively regulated by RyhB (Massé and Gottesman, 2002; Massé *et al*, 2005) for the presence of 'iron-responsive codons'. This analysis revealed that consecutive UNN codons and/or 'iron-responsive/rare codon arrangements' are predominantly found at or close to the 5′-end of these genes (data not shown). To gain further support for iron-responsive decoding, we finally tested whether the synthesis of FeSOD (*sodB*), aconitase A (*acnA*) and malate dehydrogenase (*mdh*) is affected in the *ryhB−* strain upon addition of the iron chelator. In contrast to the *sodB* and *acnA* genes, the *mdh* gene, encoding the non-iron-containing malate dehydrogenase does not contain iron-responsive codons in the 5′-coding region (Supplementary Figure S4). The synthesis of the corresponding FeSODΦLacZ and AcnAΦLacZ proteins decreased upon iron limitation in the absence of RyhB, whereas synthesis of the MdhΦLacZ protein continued unabated (Supplementary Figure S4). These results underlined our hypothesis of iron-responsive decoding and could suggest a link between iron availability and synthesis of iron-containing proteins, which are non-essential under iron-limiting conditions.

Discussion

Originally, translational coupling has been suggested to provide a mechanism to ensure equimolar synthesis of proteins encoded by a polycistronic transcript (Oppenheim and Yanofsky, 1980). In majority of examples, ribosomes terminating on the proximal gene usually relieve an inhibitory mRNA structure occluding the downstream rbs, as it appears to be the case for the *fur* gene (see Figure 2). This can either lead to *de novo* translation initiation or translational restarts (Ivey-Hoyle and Steege, 1992). Translation of *fur* required upstream translation of *uof*, and *uof* and *fur* are translated with the same ratio (see Figure 3C). Therefore, translational restarts at *fur* rather than *de novo* initiation would explain the high-efficiency translational coupling between *uof* and *fur*. Although it remains elusive as to why *fur* translation in *E. coli* K12 is regulated by means of translational coupling, it seems worth noting that an identical genetic overlap between *uof* and *fur* is found in a pathogenic *E. coli* strain as well as in

several other enteric bacteria (Figure 6). A BLAST search did not reveal any homology of the peptide encoded by *uof*, nor could any probable function be assigned by bioinformatic analyses. However, as *uof* expression is apparently regulated by iron, at present we cannot exclude the possibility that the encoded basic peptide has a role in iron metabolism.

The *in vitro* and *in vivo* experiments presented in Figure 4 showed that RyhB diminishes translation of *uof* in an Hfq-dependent manner. As *uof* and *fur* translations are coupled, to our knowledge, this is the first report on indirect translational regulation by a *trans*-encoded ncRNA. The sequence of RyhB is conserved in *E. coli* 0157:H7, *Shigella flexneri* (Oglesby *et al*, 2005) as well as in other *Shigella* species (Figure 6). In addition, an RyhB homologue with the potential to base-pair with the translation initiation region of the short reading frame upstream of *fur* gene is present in *S. enterica* (Figure 6). Thus, the molecular mechanisms underlying control of *fur* expression appear to be conserved in several enteric bacteria. In addition, the Fur-regulated RyhB orthologs of *Pseudomonas aeruginosa* (Wilderman *et al*, 2004) and *Vibrio cholerae* (Davis *et al*, 2005) display complementarity with the translation initiation region of the respective *fur* genes (B Večerek, unpublished), and thus could similarly downregulate *fur* mRNA translation (Figure 6). Yet another variation of the post-transcriptional regulation of *fur* appears to be operative in the *Anabaena* species PCC 7120. Here, a *cis*-antisense RNA has been implicated in the post-transcriptional regulation of *fur* (Figure 6; Hernandez *et al*, 2006).

RyhB apparently counterbalances the increased transcription of *uof-fur* mRNA (Figure 1) under iron-deplete conditions, that is, in the absence of metallo-Fur. One of the best-characterized mechanisms underlying the functional inactivation of a target mRNA by an ncRNA is the RyhB-mediated decay of the *E. coli sodB* mRNA. Recent work (Massé *et al*, 2003; Afonyushkin *et al*, 2005) has shown
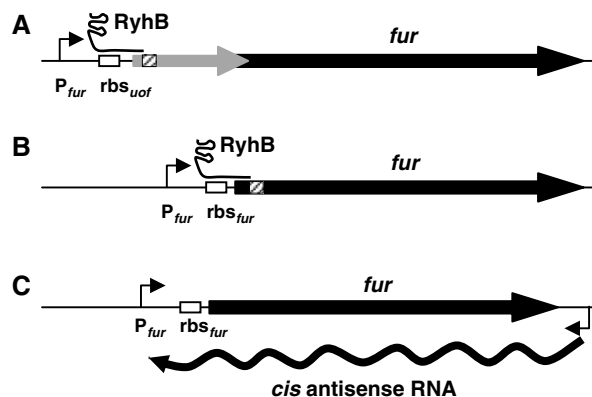
Figure 6 Established and inferred post-transcriptional control of *fur* in different bacterial species. (**A**) *E. coli* K12-like conserved regulation based on the presence of an *uof* (gray arrow), an RyhB homolog and 'iron-responsive/rare codon arrangements' (hatched rectangles) in *E. coli* 0157:H7 (GenBank NC_000913.2), four *Shigella* species (*S. dysenteriae*, GenBank CP00034; *S. boydii*, CP000036.1; *S. sonnei*, CP000038.1; *S. flexneri*, AE014073.1) and in *S. enterica* (GenBank NC_004631). (**B**) Inferred direct negative regulation of *fur* by RyhB orthologs and 'iron-responsive/rare codon arrangements' (hatched rectangles) in *P. aeruginosa* (Wilderman *et al*, 2004) and *V. cholerae* (Davis *et al*, 2005). (**C**) Putative downregulation of the *fur* gene by a *cis*-antisense RNA (wavy line) in *Anabaena* species PCC7120 (Hernandez *et al*, 2006).

that RNase E is involved in the stability control of *sodB* mRNA upon translational inhibition by RyhB. We observed that the entire *uof-fur* transcript is stabilized in RNase E mutants under non-permissive conditions (I Moll and B Večerek, unpublished). The stability of *uof-fur* mRNA was reduced in the presence of RyhB (Figure 1), and elimination of the *uof* translation initiation signals, that is, inhibition of *fur* translation (see Figure 3C), resulted in strongly diminished steady levels, as well as in a reduced stability of the $uof_{UA-CUG}fur$ mRNA *in vivo* (Supplementary Figure S2). Hence, a simple model for RyhB-mediated negative regulation of *fur* mRNA (Figure 7) would include translational inhibition of *uof-fur* translation, endonucleolytic RNase E cleavages in the untranslated *uof-fur* mRNA, followed by $3' \rightarrow 5'$ decay of intermediate mRNA fragments.

The iron–sulfur protein MiaB methylthiolates i^6A37 in certain tRNAs (Esberg *et al*, 1999; Pierrel *et al*, 2002). The conversion of i^6A37 to ms^2i^6A37 does not occur during growth of *E. coli* in iron-restricted medium (Buck and Griffiths, 1982; Buck and Ames, 1984). Under these conditions, the activity of two enzymes encoded by the *trp* operon was shown to be upregulated 2–3-fold (Buck and Griffiths,

1982). These effects were later ascribed to an increased slowing or stalling of ribosomes at the two tandem Trp codons in the leader sequence (Landick *et al*, 1990). In our studies, iron limitation resulted in a reduced expression of the 'wild-type' *uof-lacZ* gene, but not when the UCA_6 codon was replaced by UCU or when the rare AGA_7 codon was replaced by the frequently used CGU codon. The latter two variation controls showed that iron depletion does not have a general negative effect on the expression of the *uof-lacZ* gene. In addition, as the combination of the 'iron-responsive' (UCA_6) and 'rare codon' (AGA_7), but not the presence of either codon alone, resulted in a decrease in translation, effects related to plasmid-mediated overexpression of the fusion genes, that is, to a shortage of either tRNA species, can most likely be excluded. Moreover, when compared with the uof_5-*lacZ* mRNA, the presence of the sub-sequence -5'-…UCA_6AGA_7…-3' in uof_7-*lacZ* mRNA had no effect on expression in a *miaB*+ strain, but decreased expression in an *miaB*− strain (Figure 5C). As the steady-state levels of the uof_5-*lacZ* and uof_7-*lacZ* mRNAs were indistinguishable in either strain (Figure 5C), this phenomenon is most likely linked to MiaB and occurs at the level of translation.
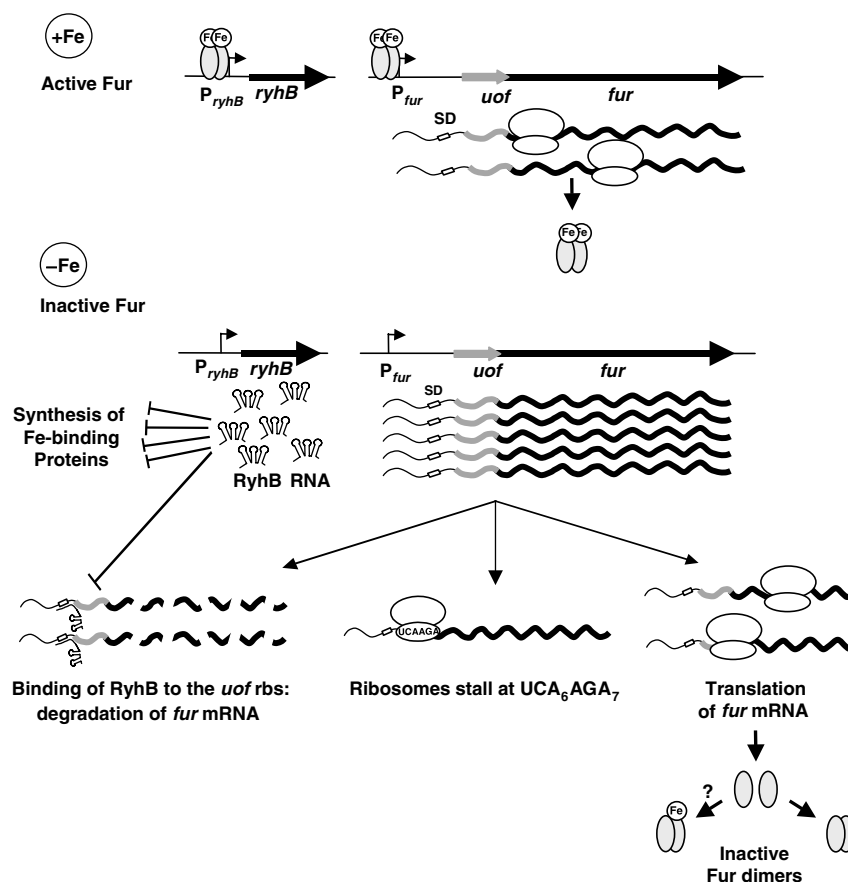
Figure 7 Model for post-transcriptional regulation of *fur* in *E. coli* K12. In the presence of iron (+Fe), metallo-Fur functions as a weak repressor of its own mRNA (De Lorenzo *et al*, 1988). As a consequence, transcription of *fur* mRNA leads to a certain level of metallo-Fur synthesis, which among many other genes represses *ryhB* transcription (Massé and Gottesman, 2002). In the absence of iron (−Fe), Fur is inactive, RyhB is synthesized and binds to and inhibits translation of multiple targets, including a number of mRNAs encoding iron-binding proteins as well as of *uof*. This results in downregulation of *uof* translation and degradation of a proportion of *uof-fur* mRNA (see Figure 1). Another level of regulation entails under-modification of $tRNA_{IV}^{Ser}$ caused by iron scarcity and the presence of the 'iron-responsive/rare codon arrangement' in *uof*. Iron-responsive decoding may serve as a back-up mechanism for RyhB-mediated regulation, and may cause a blockage of ribosomal movement and/or a release of ribosomes. The mechanisms governing post-transcriptional control of *fur* expression lead to a constant level of Fur synthesis under iron-replete and iron-deplete conditions. Inactive apo-Fur could potentially poison metallo-Fur (see text).

Surprisingly, iron-responsive decoding was observed rather rapidly (between 5 and 10 min; see Figure 5B) after addition of the iron chelator. Although there are no literature data on MiaB concerning the loss of the $[Fe–S]^{2+}$ cluster upon iron removal, it has been reported that aconitase B, which contains four $[Fe–S]^{2+}$ clusters, is very rapidly ($t_{1/2} = <5$ min) demetallated upon addition of dip (Varghese *et al*, 2003). As on the other hand the pool of tRNAs containing the ms^2i^6A modification is known to be very low under aerobic growth conditions (Buck and Ames, 1984), a rapid demetallation of MiaB upon iron shortage would be expected to lead concomitantly to a quick depletion of methylthiolated tRNAs. In turn, this could explain why iron-responsive decoding occurs rather rapidly after iron deprivation.

Previous studies have shown that hypomodification of A37 can cause +1 frameshifts (Urbonavicius *et al*, 2001). However, β-galactosidase activity conferred by the −1 and +1 out-of frame *uof-lacZ* fusions did not increase upon addition of the iron chelator (B Večerek, unpublished), which argued against a frameshifting event occurring at the sub-sequence 5′-…UCA_6AGA_7…-3′. Therefore, the observed effects can either be reconciled with ribosome stalling (Landick *et al*, 1990; Figure 7) or with mRNA/peptidyl-tRNA drop-off at the sub-sequence -5′-…UCA_6AGA_7…-3′ (Gao *et al*, 1997; Cruz-Vera *et al*, 2004). Nevertheless, as *uof* and *fur* are translationally coupled, either event would have the same consequence, that is, a decrease in Fur synthesis. Iron responsive expression of *uof-fur* may not be limited to *E. coli* K12. Assuming a similar codon usage and perhaps tRNA modification function in Gram-negative bacteria (Daniels *et al*, 1998), it is noteworthy that apart from the four *Shigella* species and *E. coli* 0157:H7 (Figure 6), comprising at the sequence level identical *uof-fur* entities, 'iron-responsive/rare codon arrangements' are also present at the beginning of the short putative reading frame upstream of *fur* in *S. enterica* as well as in the 5′-coding region of the *fur* genes of *P. aeruginosa* and *V. cholerae* (Figure 6).

In the model shown in Figure 7, RyhB-dependent silencing of *uof* concurrently with *fur* under iron-deplete conditions counterbalances *fur* mRNA synthesis transcribed in default of metallo-Fur. As a result, Fur synthesis remains steady upon iron depletion (see Figure 5A). This finding may be explained in terms of the iron-sparing model (Massé *et al*, 2005), which predicts a RyhB-mediated redistribution of intracellular iron upon repression of non-essential iron-containing proteins to essential iron-containing enzymes during iron limitation. Hence, an increase in Fur levels under these conditions could be adverse, as Fur could compete for intracellular iron with the essential iron-containing enzymes. Consequently, this scenario could interfere with sufficient iron uptake.

Iron depletion in the absence of RyhB resulted first in an increase and then a decrease of Fur translation (Figure 5A). As *fur* mRNA levels continued to increase under these conditions (Figure 1A), the decrease in the *de novo* synthesis of Fur can most likely be attributed to iron-responsive decoding. As mentioned above, MiaB inactivation may occur rapidly after iron depletion. Hence, we hypothesize that iron-responsive decoding of *uof-fur*, and by inference that of other genes (see Supplementary Figure S4), serves in addition to RyhB as a back-up mechanism to downregulate the synthesis of Fur

and other non-essential iron-containing proteins during iron limitation (Figure 7).

Why does Fur synthesis occur (Figure 7) upon iron limitation? Possibly, ongoing Fur synthesis could ensure a rapid conversion of inactive apo-Fur, synthesized during iron limitation, into metallo-Fur, and thus a quick response to reach iron homeostasis. However, any model for *fur* regulation should address the cellular abundance of Fur (Zheng *et al*, 1999). Although to our knowledge there is no direct experimental evidence, it is generally assumed that Fe^{2+} dissociates from metallo-Fur when iron becomes scarce. In light of this, we would like to suggest another possible role for the observed Fur synthesis under iron-limiting conditions. Fur binds as a dimer to DNA, and iron binding to Fur appears to trigger conformational changes, which are required for a tight interaction with the 'Fur-boxes' on DNA (Gonzalez de Peredo *et al*, 2001). However, as apo-Fur dimers have been detected, iron does not seem to be a pre-requisite for dimerization of Fur (Adrait *et al*, 1999). Taking this in consideration, it is conceivable that apo-Fur present or synthesized upon iron limitation (Figure 7) binds to residual metallo-Fur by dimerization, which in turn could lead to non-functional dimers, and thus, to an accelerated uptake of iron.

Materials and methods

Bacterial strains and plasmids
The *E. coli* strains DJ480, DJ480Δ*ryhB* (Massé and Gottesman, 2002), MC4100 and its derivative AM111 (MC4100*hfq*−) (Tsui *et al*, 1994), as well as TX3346*miaB*− (Esberg *et al*, 1999), have been described. *E. coli* strain H1941Δ*fur* was obtained from Dr K Hantke, University of Tübingen. Cells were grown at 37°C in M9 medium supplemented with 0.2% glucose, 2 mM $MgSO_4$, 0.1 mM $CaCl_2$ and 10 μg/ml thiamine. For growth of TX3346, the M9 medium was additionally supplemented with 0.05% casamino acids (Difco). Ampicillin (100 μg/ml), kanamycin (25 μg/ml) or chloramphenicol (15 μg/ml) was added to the medium where appropriate.

The construction of plasmids serving as templates for *in vitro* mRNA synthesis (see Figure 3B) and that of plasmids used to monitor *uof-lacZ*, *fur-lacZ*, *acnA-lacZ*, *sodB-lacZ* and *mdh-lacZ* expression, respectively, as well as that of plasmid variants (see Figures 3, 4 and 5) is described in Supplementary data. Transcription of the fusion genes was controlled by the *lacpo* instead of the natural *fur* promoter in plasmids used to monitor *in vivo uof-lacZ* or *fur-lacZ* expression upon addition of dip. This was performed to study regulatory events at the post-transcriptional level, that is, to avoid overlapping regulatory effects resulting from iron depletion on expression of the respective fusion genes. The copy numbers of all isogenic plasmids used in the *in vivo* experiments were found to be identical (not shown).

RNA preparation for in vitro studies
For synthesis of full-length *fur* mRNA and variants thereof, the plasmids pUuof_AUGfur, pUuof_UA-CUGfur, pUuof_5fur, pUuof_73fur or pUuof_AUGfur-inv were linearized with *Eco*RI and used as templates for *in vitro* transcription with T7 RNA polymerase (Promega). *In vitro* transcription of plasmid pUuof_AUGfur linearized with *Dra*I generated *fur242* mRNA, comprising nucleotides −183 to +59, which was used for toeprinting (see below). RyhB, RyhBΔ2 and RyhB-inv RNAs were transcribed with T7 polymerase using plasmids pURyhB, pURyhBΔ2 and pURyhB-inv (Večerek *et al*, 2003) cleaved with *Dra*I. RyhBΔ3 was transcribed using plasmid pURyhBΔ3 (see Supplementary data), after cleavage with *Sma*I. DsrA RNA (Sledjeski *et al*, 1996) was transcribed *in vitro* from PCR templates.

Determination of fur mRNA steady-state levels and stability
To determine the steady-state levels of *fur* mRNA, cells were grown in M9 medium to an OD_{600} of 0.5, when dip (250 μM final concentration) was added. Four-milliliter aliquots were withdrawn

at time 0 (before addition of dip) and 2, 4, 8 and 16 min thereafter, and total RNA was isolated using standard procedures. To determine *fur* mRNA stability, the strains DJ480 and DJ480Δ*ryhB* were grown in M9 medium at 37°C to an OD_{600} of 0.5. Then, rifampicin (200 μg/ml) was added and 4-ml aliquots were withdrawn at time 0, 1, 2 and 4 min after addition of rifampicin for total RNA isolation. *fur* mRNA levels were determined by primer extension with the AMV reverse transcriptase (Promega) using 5 μg of total RNA primed with the *fur*-specific 5′-end labelled oligonucleotide E29 (5′-GTCATGCGGAATC-3′), which is complementary to nts −8 to +5 of *fur* mRNA. In addition, the 5S rRNA levels (loading control) were determined using primer R25 (5′-ATGCCTGGCAGTTCCCTACT-3′). The samples were separated on an 8% polyacrylamide–8 M (PAA–8 M) urea gel. The gels were dried and exposed to a Molecular Dynamics PhosphoImager for quantitation.

In vitro translation and coupled in vitro transcription/translation

Full-length *fur* mRNA and variants thereof (4 pmol) were translated *in vitro* using an S30 extract for circular templates (Promega), which contains Hfq (Večerek *et al*, 2003). Plasmid pRuof-lacZ was used as a template for coupled transcription/translation in the presence or absence of increasing concentrations of RyhB and DsrA RNAs, as specified in Figure 4B. Upon incubation for 20 min at 37°C in the presence of 6 μM ^{14}C-lysine (309 mCi/mmol, Amersham Pharmacia Biotech), translation was stopped by the addition of four volumes of 90% acetone. The samples were resuspended in SDS–protein sample buffer and loaded onto a 12% SDS–polyacrylamide gel. Gels were dried and exposed to a Molecular Dynamics PhosphoImager for visualization.

Toeprinting analysis

The toeprinting assays on *fur*242 mRNA were carried out using purified 30S ribosomal subunits and initiator-tRNA, tRNA$_f^{Met}$, essentially as described by Hartz *et al* (1988). Briefly, ^{32}P-5′end-labelled oligonucleotide complementary to nucleotides +41 to +56 of *fur* mRNA served as the primer for cDNA synthesis. *fur*242 mRNA (0.04 pmol) were incubated for 5 min at 37°C in the absence (extension) and presence of 2 pmol 30S subunits (binary complex), and of 2 pmol 30S and 10 pmol tRNA$_f^{Met}$ (ternary complex), respectively, before addition of MMLV reverse transcriptase and dNTPs. The samples were separated on an 8% PAA–8M urea gel and the extension signals were visualized using a Molecular Dynamics PhosphoImager.

β-galactosidase assays

The different strains were incubated at 37°C in M9 minimal medium. At an OD_{600} of 0.5, dip (250 μM final concentration) was added to the culture. At time 0 and 5, 10 and 20 min after addition of dip, triplicate samples were withdrawn and β-galactosidase activities were determined as described elsewhere, and then averaged.

In vivo synthesis of the FurΦLacZ, UofΦLacZ and Fur proteins

Strains were grown in M9 medium at 37°C to an OD_{600} of 0.5. Then, 250 μM dip (final concentration) was added and 1 ml samples were withdrawn before addition and at different times (see Figures) after addition of the chelator. Pulse labeling was performed by the addition of 1 μl [^{35}S]methionine (10 mCi/ml, Amersham Pharmacia Biotech) for 2 min at 37°C, and then cold methionine (10 mM final concentration) was added. Upon precipitation with 5% TCA, the pellets were washed with cold acetone (90%), resuspended in protein sample buffer and boiled for 5 min before loading onto a 12% SDS–polyacrylamide gel. For determination of the relative *de novo* synthesis of the FurΦLacZ and UofΦLacZ proteins (Figure 3C, lanes 2 and 6 and Figure 5B) the Phosphoimager signals corresponding to fusion proteins were normalized to the total counts obtained from the corresponding lane.

De novo-synthesized Fur protein (Figure 5A) was visualized with rabbit anti-Fur antibodies upon blotting of the gel-separated labeled proteins onto a nitrocellulose membrane employing standard procedures. The same membrane was then subjected to autoradiography and the signals obtained with anti-Fur antibody were merged with those obtained by autoradiography to identify *de novo* synthesized Fur protein.

Translational efficiency of uof₅-lacZ and uof₇-lacZ

The MC4100 *miaB*+ and TX3346*miaB*$^-$ strains carrying plasmids pRuof₅-lacZ and pRuof₇-lacZ, respectively, were cultivated in M9 medium. At an OD_{600} of 0.5, triplicate aliquots were taken for the β-galactosidase assays. In parallel, samples were withdrawn for isolation of total RNA to determine the respective *uof₅-lacZ* and *uof₇-lacZ* mRNA levels. β-Galactosidase activities obtained with the pRuof₅-lacZ and pRuof₇-lacZ constructs of two independent experiments were averaged. The steady-state *uof₅-lacZ* and *uof₇-lacZ* mRNA levels were determined by primer extension with AMV reverse transcriptase (Promega) using 5 μg of total RNA primed with the *lacZ*-specific 5′-end labeled probe (5′-GGGAAGGGCGAT CGGT-3′). 5S rRNA, the levels of which were determined using primer R25 (see above), was used as loading control.

Supplementary data

Supplementary data are available at *The EMBO Journal* Online (http://www.embojournal.org).

References

Adrait A, Jacquamet L, Le Pape L, Gonzalez de Peredo A, Aberdam D, Hazemann JL, Latour JM, Michaud-Soret I (1999) Spectroscopic and saturation magnetization properties of the manganese- and cobalt-substituted Fur (ferric uptake regulation) protein from *Escherichia coli*. *Biochemistry* **38:** 6248–6260

Afonyushkin T, Večerek B, Moll I, Bläsi U, Kaberdin VR (2005) Both RNase E and RNase III control the stability of *sodB* mRNA upon translational inhibition by the small regulatory RNA RyhB. *Nucleic Acids Res* **33:** 1678–1689

Argaman L, Hershberg R, Vogel J, Bejerano G, Wagner EG, Margalit H, Altuvia S (2001) Novel small RNA-encoding genes in the intergenic regions of *Escherichia coli*. *Curr Biol* **11:** 941–950

Bläsi U, Nam K, Hartz D, Gold L, Young R (1989) Dual translational initiation sites control function of the lambda S gene. *EMBO J* **8:** 3501–3510

Bouadloun F, Srichaiyo T, Isaksson LA, Björk GR (1986) Influence of modification next to the anticodon in tRNA on codon context sensitivity of translational suppression and accuracy. *J Bacteriol* **166:** 1022–1027

Braun V (2005) Bacterial iron transport related to virulence. *Contrib Microbiol* **12:** 210–233

Buck M, Ames BN (1984) A modified nucleotide in tRNA as a possible regulator of aerobiosis: synthesis of *cis*-2-methyl-thioribosylzeatin in the tRNA of *Salmonella*. *Cell* **36:** 523–531

Buck M, Griffiths E (1982) Iron mediated methylthiolation of tRNA as a regulator of operon expression in *Escherichia coli*. *Nucleic Acids Res* **10:** 2609–2624

Cruz-Vera LR, Magos-Castro MA, Zamora-Romo E, Guarneros G (2004) Ribosome stalling and peptidyl-tRNA drop-off during translational delay at AGA codons. *Nucleic Acids Res* **32:** 4462–4468

Daniels C, Vindurampulle C, Morona R (1998) Overexpression and topology of the *Shigella flexneri* O-antigen polymerase (Rfc/Wzy). *Mol Microbiol* **28:** 1211–1222

Davis BM, Quinones M, Pratt J, Ding Y, Waldor MK (2005) Characterization of the small untranslated RNA RyhB and its regulon in *Vibrio cholerae*. *J Bacteriol* **187:** 4005–4014

De Lorenzo V, Herrero M, Giovannini F, Neilands JB (1988) Fur (ferric uptake regulation) protein and CAP (catabolite-activator protein) modulate transcription of *fur* gene in *Escherichia coli*. *Eur J Biochem* **173:** 537–546

Delany I, Spohn G, Pacheco AB, Ieva R, Alaimo C, Rappuoli R, Scarlato V (2002) Autoregulation of *Helicobacter pylori* Fur revealed by functional analysis of the iron-binding site. *Mol Microbiol* **46:** 1107–1122

Esberg B, Björk GR (1995) The methylthio group (ms2) of N6-(4-hydroxyisopentenyl)-2-methylthioadenosine (ms2io6A) present next to the anticodon contributes to the decoding efficiency of the tRNA. *J Bacteriol* **177:** 1967–1975

Esberg B, Leung HC, Tsui HC, Björk GR, Winkler ME (1999) Identification of the miaB gene, involved in methylthiolation of isopentenylated A37 derivatives in the tRNA of *Salmonella typhimurium* and *Escherichia coli*. *J Bacteriol* **181:** 7256–7265

Escolar L, Perez-Martin J, de Lorenzo V (1999) Opening the iron box: transcriptional metalloregulation by the Fur protein. *J Bacteriol* **181:** 6223–6229

Gao W, Tyagi S, Kramer FR, Goldman E (1997) Messenger RNA release from ribosomes during 5′-translational blockage by consecutive low-usage arginine but not leucine codons in *Escherichia coli*. *Mol Microbiol* **25:** 707–716

Geissmann TA, Touati D (2004) Hfq, a new chaperoning role: binding to messenger RNA determines access for small RNA regulator. *EMBO J* **23:** 396–405

Gonzalez de Peredo A, Saint-Pierre C, Latour JM, Michaud-Soret I, Forest E (2001) Conformational changes of the ferric uptake regulation protein upon metal activation and DNA binding; first evidence of structural homologies with the diphtheria toxin repressor. *J Mol Biol* **310:** 83–91

Grosjean H, Nicoghosian K, Haumont E, Soll D, Cedergren R (1985) Nucleotide sequences of two serine tRNAs with a GGA anticodon: the structure-function relationships in the serine family of *E. coli* tRNAs. *Nucleic Acids Res* **13:** 5697–5706

Hantke K (1984) Cloning of the repressor protein gene of iron-regulated systems in *Escherichia coli* K12. *Mol Gen Genet* **197:** 337–341

Hantke K (2001) Iron and metal regulation in bacteria. *Curr Opin Microbiol* **4:** 172–177

Hartz D, McPheeters DS, Traut R, Gold L (1988) Extension inhibition analysis of translation initiation complexes. *Methods Enzymol* **164:** 419–425

Hernandez JA, Muro-Pastor AM, Flores E, Bes MT, Peleato ML, Fillat MF (2006) Identification of a *furA cis* antisense RNA in the cyanobacterium *Anabaena sp.* PCC 7120. *J Mol Biol* **355:** 325–334

Ivey-Hoyle M, Steege DA (1992) Mutational analysis of an inherently defective translation initiation site. *J Mol Biol* **224:** 1039–1054

Kadner RJ (2005) Regulation by iron: RNA rules the rust. *J Bacteriol* **187:** 6870–6873

Landick R, Yanofsky C, Choo K, Phung L (1990) Replacement of the *Escherichia coli trp* operon attenuation control codons alters operon expression. *J Mol Biol* **216:** 25–37

Lim VI (1997) Analysis of interactions between the codon–anticodon duplexes within the ribosome: their role in translation. *J Mol Biol* **266:** 877–890

Massé E, Escorcia FE, Gottesman S (2003) Coupled degradation of a small regulatory RNA and its mRNA targets in *Escherichia coli*. *Genes Dev* **17:** 2374–2383

Massé E, Gottesman S (2002) A small RNA regulates the expression of genes involved in iron metabolism in *Escherichia coli*. *Proc Natl Acad Sci USA* **99:** 4620–4625

Massé E, Vanderpool CK, Gottesman S (2005) Effect of RyhB small RNA on global iron use in *Escherichia coli*. *J Bacteriol* **187:** 6962–6971

Morita T, Mochizuki Y, Aiba H (2006) Translational repression is sufficient for gene silencing by bacterial small noncoding RNAs in the absence of mRNA destruction. *Proc Natl Acad Sci USA* **103:** 4858–4863

Oglesby AG, Murphy ER, Iyer VR, Payne SM (2005) Fur regulates acid resistance in *Shigella flexneri* via RyhB and *ydeP*. *Mol Microbiol* **58:** 1354–1367

Oppenheim DS, Yanofsky C (1980) Translational coupling during expression of the tryptophan operon of *Escherichia coli*. *Genetics* **95:** 785–795

Pavlov MY, Freistroffer DV, MacDougall J, Buckingham RH, Ehrenberg M (1997) Fast recycling of *Escherichia coli* ribosomes requires both ribosome recycling factor (RRF) and release factor RF3. *EMBO J* **16:** 4134–4141

Pierrel F, Björk GR, Fontecave M, Atta M (2002) Enzymatic modification of tRNAs: MiaB is an iron–sulfur protein. *J Biol Chem* **277:** 13367–13370

Sala C, Forti F, Di Florio E, Canneva F, Milano A, Riccardi G, Ghisotti D (2003) *Mycobacterium tuberculosis* FurA autoregulates its own expression. *J Bacteriol* **185:** 5357–5362

Sledjeski DD, Gupta A, Gottesman S (1996) The small RNA, DsrA, is essential for the low temperature expression of RpoS during exponential growth in *Escherichia coli*. *EMBO J* **15:** 3993–4000

Tsui HC, Leung HC, Winkler ME (1994) Characterization of broadly pleiotropic phenotypes caused by an *hfq* insertion mutation in *Escherichia coli* K-12. *Mol Microbiol* **13:** 35–49

Urbonavicius J, Qian Q, Durand JM, Hagervall TG, Björk GR (2001) Improvement of reading frame maintenance is a common function for several tRNA modifications. *EMBO J* **20:** 4863–4873

Varghese S, Tang Y, Imlay JA (2003) Contrasting sensitivities of *Escherichia coli* aconitases A and B to oxidation and iron depletion. *J Bacteriol* **185:** 221–230

Večerek B, Moll I, Afonyushkin T, Kaberdin V, Bläsi U (2003) Interaction of the RNA chaperone Hfq with mRNAs: direct and indirect roles of Hfq in iron metabolism of *Escherichia coli*. *Mol Microbiol* **50:** 897–909

Wilderman PJ, Sowa NA, FitzGerald DJ, FitzGerald PC, Gottesman S, Ochsner UA, Vasil ML (2004) Identification of tandem duplicate regulatory small RNAs in *Pseudomonas aeruginosa* involved in iron homeostasis. *Proc Natl Acad Sci USA* **101:** 9792–9797

Zheng M, Doan B, Schneider TD, Storz G (1999) OxyR and SoxRS regulation of *fur*. *J Bacteriol* **181:** 4639–4643